Effective tunneling processes in an interferometer of helical edge states with an antidot

2014 J. Phys.: Conf. Ser. 568 052027

(http://iopscience.iop.org/1742-6596/568/5/052027)

Journal of Physics: Conference Series **568** (2014) 052027 doi:10.1088/1742-6596/568/5/052027

Effective tunneling processes in an interferometer of helical edge states with an antidot

Bruno Rizzo

Departamento de Fisica and IFIBA, Facultad de Ciencias Exactas y Naturales, Universidad de Buenos Aires, Pab. I, Ciudad Universitaria, 1428 Buenos Aires, Argentina

Alberto Camjayi

Departamento de Fisica and IFIBA, Facultad de Ciencias Exactas y Naturales, Universidad de Buenos Aires, Pab. I, Ciudad Universitaria, 1428 Buenos Aires, Argentina

Liliana Arrachea

Departamento de Fisica and IFIBA, Facultad de Ciencias Exactas y Naturales, Universidad de Buenos Aires, Pab. I, Ciudad Universitaria, 1428 Buenos Aires, Argentina

Abstract. We consider an interferometer of edge states of a two-dimensional topological insulator with an antidot. We analyze the mechanisms leading to an effective tunneling with spin flip between different helical states.

1. Introduction

Recent experiments in quantum wells of the two-dimensional topological insulator HgTe demonstrated a dissipationless charge transport through its helical edge states (HES) [1, 2, 3]. Due to the time reversal symmetry that holds in this material, the edge states come in Kramer's pairs [4, 5, 6], through which the electrons move with a defined spin associated with the direction of propagation [7].

The nature of the electron propagation in HES along with the topological protection against backscattering, make these materials very appealing to be employed for spintronics and quantum computation [8, 9]. This motivates the study of configurations of helical interferometers in setups including voltages and constrictions akin to those fabricated with quantum Hall edge states [10, 11, 12, 13, 14, 15, 16, 17, 18, 19]. So far, most of the studies were based on scattering at quantum point contacts connecting two HES [10, 11, 12, 13, 14, 16, 17, 19], while the effect of a wide tunnelling contact was also recently analyzed [15, 18]. Quite generally, the (local) time-reversal invariance only allows for the direct scattering between edge states situated at different sides of the sample, while the direct (back) scattering within the same Kramer's pair is forbidden even in the presence of a constriction. Therefore, the scattering at the point contact is characterized by two parameters, one describing a spin-preserving tunneling and one describing a spin-flip tunneling between two Kramer's pairs. However it is still unclear whether these effects are present in real setups. For this reason, in a previous work we have proposed a simple test

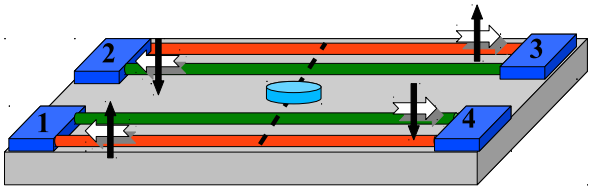

Figure 1. (Color online) Sketch of the helical edge states of a topological insulator with an antidot in the center. The pair of edge states in contact to the voltages $V_1, \ldots, V_4$ define the terminals $l = 1, \ldots, 4$.

based on the measurement of noise, as a concrete procedure to check the presence or absence of spin-flip tunneling between HES at the quantum point contact [19].

In interferometers fabricated with edge states of a two dimensional electron gas in the quantum Hall regime, the effects introduced by antidots in the bulk of the bar have been widely studied [20]. Antidots in quantum Hall systems are generated by applying a negative voltage on a surface gate, which generates an artificial repulsive impurity and a center for many-body interactions in local contact to the edge states. A similar type of structure can be also generated in a topological insulator, as sketched in Fig.(1). The aim of this work is to analyze the effect of an antidot in generating backscattering in a Kramer's pair of helical edge states as well as providing channels for inter-pair tunneling processes.

2. Model and theoretical framework

We model the topological insulator (TI) as a bar with infinite length sketched in Fig. 1. Each longitudinal edge of the TI hosts a Kramer's pair of HES with a given helicity. This is described by a Hamiltonian of one-dimensional (1D) free electrons with a definite spin and momentum. The TI is assumed to have an antidot inserted in the center of the bar, which hybridizes with the upper and lower edge states by means of spin-preserving tunneling processes. The electron levels of the dot also correspond to a pair of HES circulating around the small region of the sample where the surface gate is applied. For simplicity we model it by a single spin-degenerate level with a Coulomb repulsion energy for double occupancy. We also consider a local spin-flip process at the dot, representing a possible local tunneling within the pair induced by the surface voltage. Thus, the electrons propagating through a given edge channel of the TI could tunnel into the dot and tunnel again into another edge channel, with a different helicity. The full Hamiltonian reads $H = H_0 + H_d + H_t$. The Hamiltonian for the HESs is

$$H_0 = -i\hbar v_F \sum_{\sigma=\uparrow,\downarrow} \int dx [: \Psi^\dagger_{R,\sigma}(x)\partial_x \Psi_{R,\sigma}(x) : - : \Psi^\dagger_{L,\overline{\sigma}}(x)\partial_x \Psi_{L,\overline{\sigma}}(x) :], \quad (1)$$

where $\overline{\sigma}$ stands for the spin opposite to σ. We have assumed that a Kramer's pair of right-moving(R) with $\uparrow$ spin electron states and left-moving (L) with $\downarrow$ spin ones lie along the top edge of the bar, while another pair $L, \uparrow$ and $R, \downarrow$ lie on the bottom, as shown in Fig 1. The Fermi velocity v_F is assumed to be the same for the two pairs and $: O :$ denotes normal ordering.

The antidot (impurity) is described by the following Hamiltonian

$$H_d = \sum_{\sigma=\uparrow,\downarrow} \left[\varepsilon_0 d_\sigma^\dagger d_\sigma + \frac{U}{2} n_\sigma n_{\overline{\sigma}} + R d_\sigma^\dagger d_{\overline{\sigma}} \right], \tag{2}$$

with ε_0 is the single energy level, $n_\sigma = d_\sigma^\dagger d_\sigma$ and U represents the Coulomb interaction. We also consider a spin-flip scattering process inside the dot represented by the last term of Eq.(2) [21]. Finally the tunneling between the quantum dot located at x_0 and the HESs is,

$$H_t = \sum_{\alpha=R,L} \sum_{\sigma=\uparrow,\downarrow} \int dx \Gamma(x) [\Psi_{\alpha,\sigma}^\dagger(x) d_\sigma + H.c.], \tag{3}$$

where $\Gamma(x) = \sqrt{a}\gamma\delta(x - x_0)$ and a is a characteristic length of the coupling region between the antidot and the HESs.

The current operator for electrons flowing into the terminal l reads $\hat{I}^l(x) = ev_F \left[\hat{\rho}_+^l(x) - \hat{\rho}_-^l(x) \right]$, where $\hat{\rho}_+^l(x)$ is the density operator for particles incoming (outgoing) $l+$ ($l-$) the terminal l. The associated indices α, σ, with $\alpha = L, R$ and $\sigma = \uparrow, \downarrow$, depend on the terminal under consideration. For example, for $l = 3$, the $l+$ indices are $R, \uparrow$. The mean value of this current can be evaluated by recourse to the non-equilibrium Green's function formalism presented in Ref. [19], by introducing suitable generalizations to treat the Coulomb interaction U at the dot. We find for small bias voltage difference V at the terminals [22],

$$I^l(x) = I_0^l - I_{sp}^l - I_{sf}^l - I_b^l. \tag{4}$$

The first term, $I_0^l = \frac{e}{\hbar} \int_{-\infty}^{+\infty} \frac{d\omega}{2\pi} \left[f_{\alpha\sigma}(\omega) - f_{\overline{\alpha}\overline{\sigma}}(\omega) \right]$ is the perfect ballistic current induced in the terminal l in the absence of the tunneling to the dot. The other terms account for the contact between the HESs and the dot and tend to decrease of the current I^l with respect to the ballistic limit. We can distinguish different contributions, which describe, respectively, the tunneling to the wires in the opposite side of the bar preserving the spin (sp) and flipping the spin (sf). In addition, there is a backscattering contribution I_b^l which represents an effective resistance in the wire l. Explicitly, these terms read

$$\begin{aligned} I_{sp}^l &= \frac{e}{\hbar} \int_{-\infty}^{+\infty} \frac{d\omega}{2\pi} T_{\sigma\sigma}(\omega) \left[f_{\alpha\sigma}(\omega) - f_{\overline{\alpha}\sigma}(\omega) \right], \quad I_{sf}^l = \frac{e}{\hbar} \int_{-\infty}^{+\infty} \frac{d\omega}{2\pi} T_{\sigma\overline{\sigma}}(\omega) \left[f_{\alpha\sigma}(\omega) - f_{\alpha\overline{\sigma}}(\omega) \right], \\ I_b^l &= \frac{e}{\hbar} \int_{-\infty}^{+\infty} \frac{d\omega}{2\pi} T_{\sigma\overline{\sigma}}(\omega) \left[f_{\alpha\sigma}(\omega) - f_{\overline{\alpha}\overline{\sigma}}(\omega) \right], \end{aligned} \tag{5}$$

being

$$T_{\sigma\sigma'}(\omega) = (\sqrt{a}\gamma)^4 |g_{\alpha\sigma}^{0r}(\omega, x, x_0)|^2 |G_{\sigma,\sigma'}^r(\omega)|^2 \tag{6}$$

In the above expressions, $g_{\alpha\sigma}^{0,r}(x, x', \omega) = -\frac{i}{v_F\hbar} \Theta\left(s_\alpha(x - x')\right) \exp\left[i \frac{\omega}{v_F\hbar}(x - x') \right]$, with $s_\alpha = +1(-1)$ if $\alpha = R(L)$, are the retarded Green's functions of the isolated helical state, while $G_{\sigma,\sigma'}^r(\omega)$ is the Fourier transform of the retarded Green's function of the interacting dot in contact to the helical states $G_{\sigma,\sigma'}^r(t - t') = -i\Theta(t - t')\langle\{d_\sigma(t), d_{\sigma'}^\dagger(t')\}\rangle$.

3. Results

The retarded Green's function of the interacting quantum dot is calculated exactly in the non-interacting limit $U = 0$ and with quantum Monte Carlo by following the procedure of Refs. [23] in the symmetric Anderson model for finite U. In the latter case, the corresponding density of states $\rho_\sigma(\omega) = -2\mathrm{Im}[G_{\sigma\sigma}^r(\omega)]$ is obtained by analytic continuation from the Matsubara to the

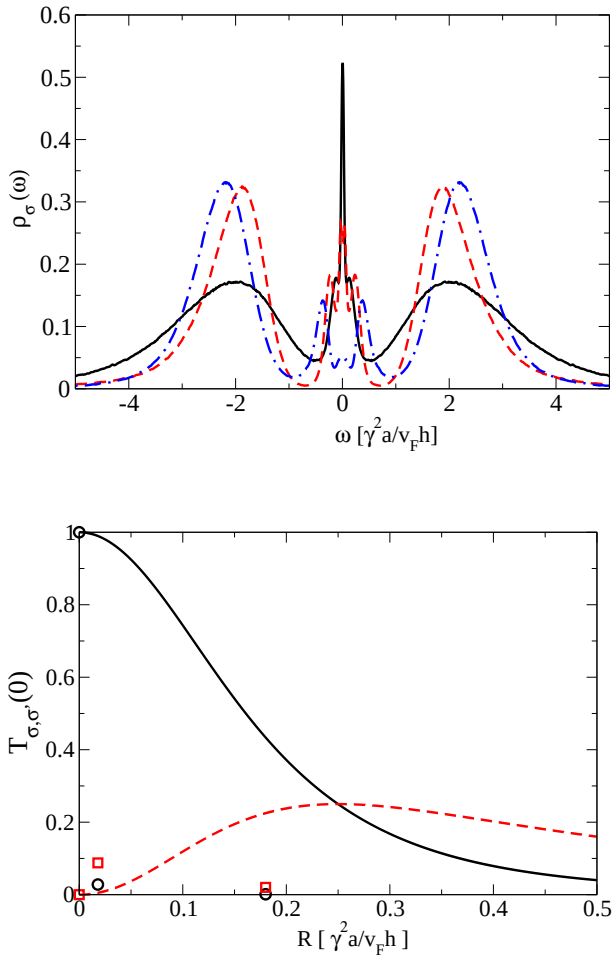

Figure 2. (Color online) a) The density of states ρ_σ ($\rho_\downarrow = \rho_\uparrow$) in the dot for three different values of spin-flip: $R = 0$ (black solid line),0.018 (red dashed line) and 0.18 (blue dashed-dotted line). $\varepsilon_0 = -U/2$, $T = 0.0025$, $U = 4$ and $\sqrt{a}\gamma = 0.5$. b) Transmission coefficient $T_{\sigma\sigma}(0)$ as functions of the amplitude of the spin-flip parameter R for $U = 0$ (black solid line) and for $U = 4$ (black open circles) and $T_{\sigma\bar{\sigma}}(0)$ as functions of R for $U = 0$ (red dashed line) and for $U = 4$ (red open squares) .

real frequency axis and typical results are shown in Fig. 2a. We see that for these parameters the Kondo peak at $\omega = 0$ is clearly distinguished for $R = 0$. The effect of R is to introduce strong spin fluctuations at the dot, which conspire against the constitution of the Kondo resonance. For this reason, the peak melts down for increasing R.

In order to study the effect of the different interactions at the dot on the transport properties of the interferometer wires, we analyze the transmission functions at the Fermi level of the wires, assumed at $\omega = 0$. Results are shown in Fig. 2b. The energy of the bare level is assumed to be $\varepsilon_0 = -U/2$, in order to have the impurity at half filling and the resonance aligned with the Fermi energy. We see that in the non-interacting case ($U = 0$), the transmission $T_{\sigma,\sigma}(0) = 1$ for $R = 0$ and decreases as this parameter increases. Instead, the transmission with spin flip shows the opposite behavior. It vanishes at $R = 0$ and increases with this parameter. We see that for $R = 0$ the behavior is the same for $U = 0$ and for $U = 4$. This is because for this value of the Coulomb interaction the dot is in the Kondo regime (see Fig. 2a) and the Kondo resonance opens a perfect transmission channel with $T_{\sigma,\sigma}(0) = 1$ and $T_{\sigma,\bar{\sigma}}(0) = 0$. For $R \neq 0$ the behavior

is, however, clearly different for both values of U. In the non-interacting case, for increasing R, the spin preserving transmission decreases as the spin-flip one increases. This is also the case for $U = 4$ and small values of R, where the Coulomb interaction seems to enhance the spin fluctuations induced by R, in comparison to the non-interacting case. However, for large enough R, the Kondo resonance decreases and tends to disappear, which means a vanishing small spin preserving transmission and a spin-flip transmission which is much smaller than the non-interacting one.

4. Summary and Conclusions

We have studied scattering effects of an antidot coupled to helical edge states of a topological insulator. We have considered a local spin-flip mechanism as well as a Coulomb interaction. We have shown that these two interactions generate relevant effects in the transmission functions that define the electron transport through the helical edge states. These processes open new possibilities in the manipulation of electron currents in topological insulator interferometers, which may be useful for generating controlled orbital entanglement similar to the one proposed in Ref. [24].

References

[1] König M, Wiedmann S, Brüne C, Roth A, Buhmann H, Molenkamp L W, Qi X L and Zhang S C 2007 *Science* **318** 766
[2] König M, Buhmann H, Molenkamp L W, T Hughes, Liu C X, Qi X L, and Zhang S-C 2008 *J. Phys. Soc. Jpn.* **77** 031007
[3] Roth A, Brüne C, Buhmann H, Molenkamp L W, Maciejko J, Qi X L, and Zhang SC 2009 *Science* **325** 294
[4] Kane C L and Mele E J 2005 *Phys. Rev. Lett.* **95** 226801
[5] Wu C, Bernevig B A and Zhang S C 2006 *Phys. Rev. Lett.* **96** 106401
[6] Xu C and Moore J 2006 *Phys. Rev. B* **73** 045322
[7] Kane C L and Mele J E 2005 *Phys. Rev. Lett.* **95** 146802
[8] Prinz G A 1998 *Science* **282** 1660
[9] Wolf S A, Awschalom D D, Buhrman R A, Daughton J M, von Molnár S, Roukes M L, Chtchelkanova A Y and Treger D M 2001 *Science* **294** 1488
[10] Hou C Y Y, Kim E A, and Chamon C 2009 *Phys. Rev. Lett.* **102** 076602
[11] Ström A and Johannesson H 2009 *Phys. Rev. Lett.* **102** 096806
[12] Teo J and Kane C L 2009 *Phys. Rev. B* **79** 235321
[13] Schmidt T L 2011 *Phys. Rev. Lett.* **107** 096602
[14] Ferraro D, Wahl C, Rech J, Jonckheere T and Martin T 2014 *Phys. Rev. B* **89** 075407
[15] Dolcetto G, Barbarino S, Ferraro D, Magnoli N and Sassetti M 2012 *Phys. Rev. B* **85** 195138
[16] Dolcini F 2011 *Phys. Rev. B* **83** 165304
[17] Romeo F, Citro R, Ferraro D, Sassetti M 2012 *Phys. Rev. B* **86** 165418
[18] Sternativo P and Dolcini F 2014 *Phys. Rev. B* **89** 035415
[19] Rizzo B, Arrachea L and Moskalets M 2013 *Phys. Rev. B* **88** 155433
[20] Sim H S, Kataoka M and Ford C J B 2007 *Phys. Rep.* **456** 127; references therein
[21] Lopez R and Sanchez D 2003 *Phys. Rev. Lett.* **90** 116602
[22] Rizzo B, Camjayi A and Arrachea L, in preparation
[23] Camjayi A and Arrachea L 2012 *Phys. Rev. B* **86** 235143 ; ibid 2014 it J. Phys.: Condens. Matter **26** 035602
[24] Rizzo B, Arrachea L and Paz J P 2012 *Phys. Rev. B* **85** 045442